High-efficiency Power Characteristics for WCDMA Applications of SiGe HBT Devices Using a Novel Form of Base-bias Resistance

M. Kondo, I. Miyashita†, M. Koshimizu†, Y. Kagotoshi†, H. Nagai†, and K. Washio

Central Research Laboratory, Hitachi, Ltd.,
1-280 Higaishi-koigakubo, Kokubunji-shi, Tokyo 185-8601, Japan
†Hitachi, Ltd., Semiconductor & Integrated Circuits,
111 Nishiyokote-machi, Takasaki-shi, Gunma, 370-0021, Japan

Abstract — **We present SiGe heterojunction bipolar transistor (HBT) devices that exhibit highly efficient and linear power characteristics comparable to those of GaAs HBTs under wide-band code-division multiple-access (WCDMA) modulation for the first time. Two resistors in series are inserted in the base-bias current path of the device. One only conducts envelope-frequency components of the base current while the other also conducts DC. By adjusting the resistance values, the adjacent channel power ratio (ACPR) was significantly reduced over a wide range of output power levels without loss of efficiency. An optimized device with a total emitter area 3390 μm^2 exhibited 44% power-added-efficiency (PAE) and 27.3-dBm output power with ACPR of less than -40 dBc under WCDMA modulation at 1.95 GHz and 3.4-V bias voltage.**

I. Introduction

Recently, SiGe HBTs have been receiving a lot of attention as devices for power amplifiers of cellular phones. They exhibit high levels of performance as RF power devices, comparable to those of GaAs HBTs [1, 2]. Moreover, they are much cheaper to implement on chips than GaAs HBTs because they are manufactured on large Si wafers by using high-yield process technologies.

To increase the application of SiGe HBT devices in cellular-phone power amplifiers, we need to obtain good power characteristics comparable to those of GaAs HBTs under modulation of third generation systems. Devices for the power amplifiers of WCDMA systems, which are representative of the 3rd generation, require low ACPR values, that is, high-linearity without loss of efficiency. Achieving this is very difficult because WCDMA systems use a wide frequency spectrum with a narrow spacing between adjacent channels. The characteristics of reported SiGe HBT power devices for WCDMA systems have not been sufficient to compete with GaAs HBTs [3].

The envelopes of the RF signals strongly affect the ACPR [4]. An envelope component at a frequency ω_2-ω_1 (~5 MHz), where ω_1 and ω_2 are adjacent channel frequencies, produces a power leakage to the adjacent channels at frequencies $2\omega_2$-ω_1 and $2\omega_1$-ω_2, due to nonlinearity of amplification.

The average of the collector current I_c for a power HBT operating in class AB varies with the envelope frequency, because the troughs of the envelope are clipped at I_c=0 (Fig. 1) [5]. The average of the base current I_b varies in the same way because of I_b's proportionality to I_c. Modulation of the average I_b would be expected to change the envelope, reducing the ACPR. To obtain this modulation, we inserted two resistors in the base-bias current path. One only conducts the envelope-frequency components of the I_b, while the other, which is similar to conventional base ballast resistors, also conducts DC. The effects of these resistors on the circuit's power characteristics are presented in detail below.

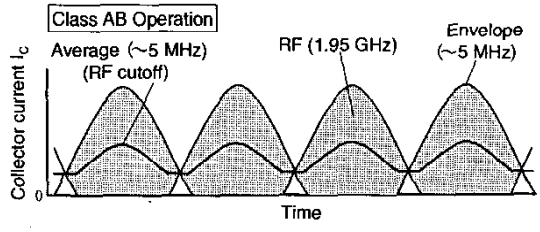

Fig. 1. Schematic view of the envelope and the average of collector current I_c over time for a HBT device in class AB operation.

II. Experimentals

Power devices with multiple SiGe HBTs were fabricated by using 0.35-μm SiGe BiCMOS process technologies. The base layer consisted of epitaxial SiGe with a uniform Ge content of 5%. Peak B concentration in the layer was 5×10^{19} cm^{-3}. The collector's Si epitaxial layer was 0.7-μm thick. Selective ion-implanted collector (SIC) technology was used to modulate the impurity concentration in the collector's intrinsic region, thus increasing the cut-off frequency, f_T. The unit cell for the devices (two 1.5×10 μm emitter fingers) exhibited

0-7803-7695-1/03/$17.00 © 2003 IEEE

h_{FE}=150, peak f_T=24 GHz, peak f_{max}=60 GHz, BV_{CEO}=5.0 V, and BV_{CBO}=15 V. Each power device consisted of 113 unit cells, for a total emitter area of 3390 μm^2.

The power characteristics were measured by a load-pull method under WCDMA modulation at 1.95 GHz with a 3.4 V bias voltage. Figure 2 shows a diagram of the circuit used. Resistors A and B were inserted in series between the DC voltage supply (Agilent 6632B) and the base of the device. The force terminal of the supply and a condenser to fix the voltage were connected to one node of resistor A, and the sense terminal was connected to the node between the two resistors, which is named node X, through an inductor of over 10 μH. The other node of resistor B, which is named node Y, was connected to the base through an RF-cutoff inductor.

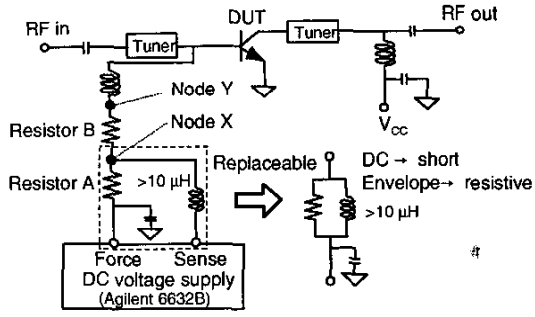

Fig. 2. Circuit configuration for the measurement.

In the voltage supply, signals from the sense terminal are passed through a low-pass filter with a cutoff frequency of several kHz. This prevents the feedback function for constant-voltage supply to the node where the sense terminal is connected from following variations at frequencies above this limit. A voltage drop across resistor A was produced by the average I_b that varied with the envelope frequencies (~5 MHz). Therefore, the voltage at node X varied with these frequencies, although the average was kept at the set value by the supply. Figure 3 is a schematic view of the time dependence of voltage at the node (Fig. 3(b)), together with the envelope and the average of I_b (Fig. 3(a)). Effectively, the DC component is short-circuited and only the envelope-frequency components pass through resistor A. Therefore, the parallel combination of resistor A and an inductor of over 10 μH to block the envelope-frequency components can replace resistor A with the feedback function of the voltage supply; that is shown as the inset of Fig. 2.

On the other hand, both the envelope-frequency components and DC component pass through resistor B, so both components contribute to the voltage drop. This drop is the same as for the equivalent resistor of the conventional configuration, i.e. the base ballast resistor. A schematic view of voltage at node Y, which is the base voltage V_{BE} with RF components being cut off, is given in Fig. 3(c) for a case with resistor A not present.

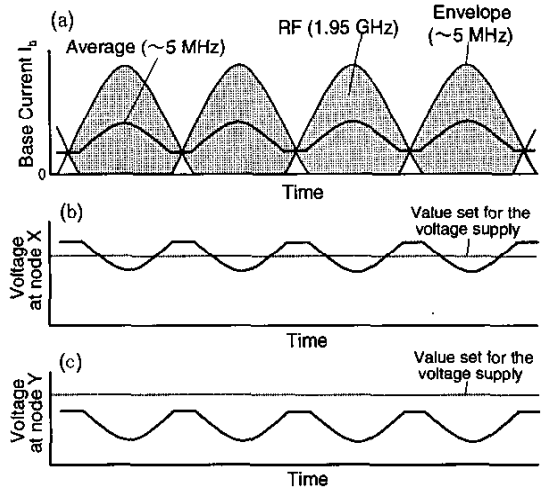

Fig. 3. Schematic view of (a) the envelope and the average of base current I_b, (b) voltage at the node between resistor A and resistor B (node X), and (c) voltage at the node between resistor B and the RF-cutoff inductor (node Y) with resistor A not present, over time, for a power-HBT device in class AB operation.

We varied the resistance values of resistor A (r_A) and resistor B (r_B) between 0 Ω and 22 Ω, and measured the resulting power characteristics. Our aims were to maximize the power-added-efficiency (PAE) and the level of output power value below which the ACPR is less than -40 dBc.

III. Results and Discussion

Figure 4 shows the effects of r_A on power characteristics, that is, the PAE, power gain G_P, ACPR-low (-5-MHz offset), and ACPR-high (+5-MHz offset) as functions of output power P_{out} for a device with r_B=0 Ω. In these cases, the voltage at node X coincides with the V_{BE} with RF components being cut off. Quiescent current, I_q, was set to 40 mA. Impedance-matching conditions were the same in all the cases, having been optimized for high PAE and low ACPR. In the case with r_A=0 Ω, both ACPR-low and ACPR-high were greater than -40 dBc over the whole range of P_{out}. They were significantly reduced for over a wide range of P_{out} by increases in r_A. The greatest reduction was in ACPR-high in the middle-range of P_{out}

values. With r_A=11 Ω, both ACPR-low and ACPR-high were below -40 dBc over the whole P_{out} range below 26.5 dBm. However, the reduction in ACPR-low at P_{out}=26 dB entered saturation when r_A was above 5 Ω, and actually increased with r_A in the higher-P_{out} range. Variation of r_A had almost no effect on the PAE and G_P characteristics.

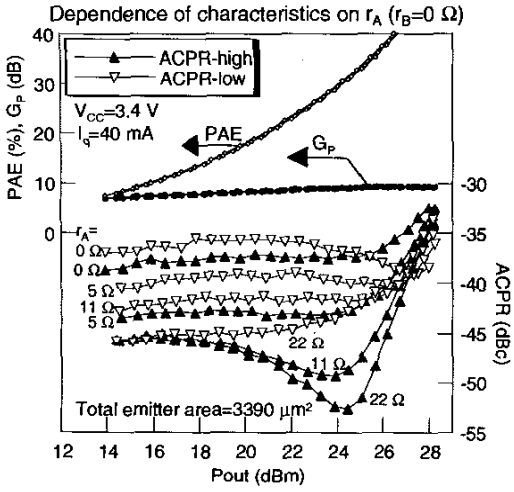

Fig. 4. The effect of r_A on power characteristics for a device with r_B=0 Ω.

We judged that the reduction in ACPR was due to the removal of distortion from the envelope of I_c which was achieved by placing a resistance in the path of the envelope-frequency components of I_b. The linearizing effect of the resistance was assumed to be responsible for reduction in exponential distortion ($I_c=I_S\exp(qV_{bc}/kT)$) [6, 7] of the envelope. In the high-P_{out} range, envelope distortion due to quasi-saturation [6] was probably relieved by the drop in V_{BE} at the upper peaks of the envelope, as shown in Fig. 3(b). The immunity of the PAE and G_P characteristics to changes in r_A was due to the fact that the bias point, that is, the DC component of the V_{BE}, was not affected by the insertion of resistor A, as is also shown in Fig. 3(b).

Figure 5 shows the effects of r_B on of the power characteristics as functions of P_{out}. Here, r_A=0 Ω. The I_q value was again set to 40 mA. ACPR-low fell with increasing r_B across a wide range of P_{out}. The size of the reductions seen with given increases in r_B were generally smaller than those seen with the same increases in r_A, although this was not the case for the higher-P_{out} range. ACPR-high values fell with increasing r_B only in the higher-P_{out} range, with the r_B value having little effect in the lower-P_{out} range. Increases in r_B led to increased PAE and decreased G_P; this is in contrast to the non-effect of increases in r_A.

In these cases, the V_{BE} falls because of the DC current component passing through resistor B (Fig. 3(c)). The changes in PAE and G_P were thus attributed to a shift in the bias point towards class-B operation. We also attributed the smallness of the changes in ACPR with r_B to this change. That is, the linearization effect obtained by having the envelope-frequency components pass through resistor B were thought to have been canceled by the change in the bias point. This is because exponential distortion increases as the mode of operation changes from class AB to class B. The variation with r_B in the dependence of G_P on P_{out} was also assumed to affect the ACPR, as has been reported in a literature [8].

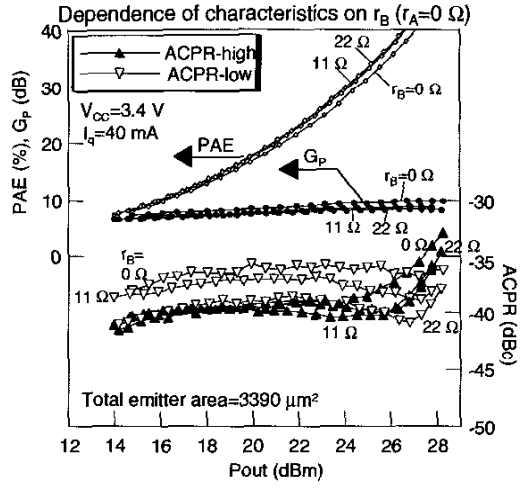

Fig. 5. The effect of r_B on power characteristics for a device with r_A=0 Ω.

The reduction rates of ACPR-low and ACPR-high at P_{out}=16 dBm and P_{out}=27 dBm with increases in r_A and r_B (0 Ω → 22 Ω) are summarized in Table I. Note the opposite patterns of relative size of the reduction rates for the cases of increases in r_A and in r_B. The reasons for this are not clear. The high ACPR-low in the high-P_{out}

TABLE I
ACPR REDUCTION RATES WITH INCREASES IN r_A AND IN r_B AT LOW AND HIGH P_{OUT} VALUES

	ACPR-low		ACPR-high	
	P_{out}=16 dBm	27 dBm	16 dBm	27 dBm
Increase in r_A (0 Ω→22 Ω)	-9.1 dB	+1.0 dB (Increase)	-7.8 dB	-5.4 dB
Increase in r_B (0 Ω→22 Ω)	-3.0 dB	-4.0 dB	-0.6 dB	-2.6 dB

range was the only serious problem in the cases where only resistor A was used. We would expect the inclusion of resistor B in series with resistor A, i.e., as shown in Fig. 2 to alleviate this problem, since strong reduction in ACPR-low were seen in this P_{out} range when only resistor B was present.

We adjusted the r_A and r_B values of the circuit shown in Fig. 2 in order to optimize its power characteristics. Results for the optimized circuit are shown in Fig. 6. PAE, G_P, ACPR-low, and ACPR-up are shown as functions of P_{out} for the case where r_A=15 Ω and r_B=10 Ω. The device exhibited PAE=44% and P_{out}=27.3 dBm with levels of both ACPR-low and ACPR-high below -40dBc, for bias voltage V_{CC}=3.4 V and I_q=40 mA. So far as we know, this is the first time that characteristics under WCDMA modulation comparable to those of GaAs HBTs have been obtained for SiGe HBT power devices. One problem that requires further counter measures was the low G_P (9 dB). This was mainly due to the magnitude of the emitter-base capacitance C_{jE}, which was several times greater than the value for a GaAs HBT with the same emitter area.

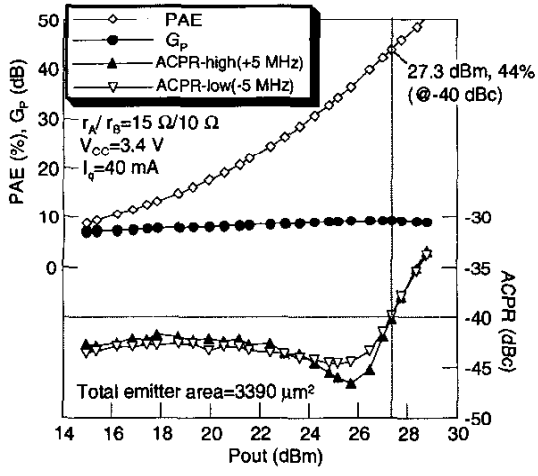

Fig. 6. Power characteristics as optimized by adjusting the resistance values of resistors A and B.

IV. Conclusions

We have presented a new approach to obtaining highly efficient and linear power characteristics for SiGe HBT devices; our intention was to make them more applicable to power amplifiers for WCDMA cellular phone systems. We include two series-connected resistors in the base-bias current path; one only conducts the envelope-frequency components, and the other also conducts the DC component. By adjusting the resistances, we significantly reduced the ACPR over a wide range of output power levels without losing efficiency. An optimized device exhibited 44% power-added-efficiency and 27.3-dBm output power with an ACPR of less than -40 dBc under WCDMA modulation at 1.95 GHz with 3.4-V bias voltage and quiescent current I_q=40 mA.

Acknowledgments

The authors are grateful to Y. Matsunaga, T. Kobori, and H. Ono for the supports in the sample preparation and the load-pull measurements, and to T. Kuramoto, N. Machida and M. Yamane for the technical discussions and the supports in the fabrication of SiGe HBTs.

References

[1] P. Tseng, L. Zhang, G. Gao, and M.F. Chang, "A 3V monolithic SiGe HBT power amplifier for dual-mode (CDMA/AMPS) cellular handset applications," *IEEE Journal of Solid-State Circuits*, vol. 35, no. 9, pp. 1338-1344, Sept. 2000.

[2] X. Zhang, C. Saycocie, S. Munro, and G. Henderson, "A SiGe HBT power amplifier with 40% PAE for PCS CDMA applications," *2000 IEEE MTT-S Int. Microwave Symposium Digest*, vol. 1, pp. 857-860, June 2000.

[3] J. Pusl, S. Sridharan, P. Antognetti, D. Helms, A. Nigam, J. Griffiths, K. Louie, and M. Doherty, "SiGe power amplifier ICs with SWR protection for handset applications," *Microwave Journal*, vol. 44, no. 6, pp. 100-113, June 2001.

[4] J. Vuolevi, "Analysis, measurement and cancellation of the bandwidth and amplitude dependence of intermodulation distortion in RF power amplifiers," Ph. D. thesis, University of Oulu, Finland, Oct. 2001.

[5] M. Nakayama, K. Horiguchi, and T. Takagi, "A study of intermodulation distortion of microwave FET for impedance of bias circuit and bias condition dependence," *Technical Report of IEICE*, vol. 97, no. 288, MW97-86, pp. 39-44, Sept. 1997 (in Japanese).

[6] L.C.N. de Vreede, W. van Noort, H.F.F. Jos, H.C. de Graaff, J.W. Slotboom, and J.L. Tauritz, "Optimum dimensions of the epilayer for third-order intermodulation distortion," *Proc. IEEE BCTM 1998*, pp. 168-171, Sept. 1998.

[7] G. Niu, Q. Liang, J.D. Cressler, C.S. Webster, and D.L. Harame, "RF linearity characteristics of SiGe HBT," *IEEE Trans. Microwave Theory Tech.*, vol. 49, no. 9, pp. 1558-1565, Sept. 2001.

[8] T. Iwai, K. Kobayashi, Y. Nakasha, T. Miyashita, S. Ohara, and K. Joshin, "42% high-efficiency two-stage HBT power-amplifier MMIC for W-CDMA cellular phone systems," *IEEE Trans. Microwave Theory Tech.*, vol. 48, no. 12, pp. 2567-2572, Dec.2000.